First Principles Investigation of H Addition and Abstraction Reactions on Doped Aluminum Clusters

David J. Henry, Adrian Varano, and Irene Yarovsky*

Applied Physics, School of Applied Sciences, RMIT University, GPO Box 2476V, Victoria 3001, Australia

Received: December 4, 2008

We have investigated axial interactions of H_2 with $Al_{12}X$ (X = Mg, Al, and Si) clusters and found that homolytic dissociation leading to $Al_{12}XH$ and H atom proceeds without a barrier but is an extremely endothermic process. The calculated difference in energy of the addition and abstraction reactions indicates that any $Al_{12}X$-based hydrogen storage technology that involves predissociation of H_2 will be limited by the competing processes. We have also discovered that while there is a modest barrier for dissociation of H_2 on a single $Al_{12}Mg$ cluster to give the dihydride, the process occurs spontaneously between two closely spaced $Al_{12}Mg$ clusters, resulting in the formation of two $Al_{12}MgH$ species. Doping of the cluster with an electropositive atom (Mg) enables the transfer of electron density to the Al cage, which enhances H_2 dissociation. The information gained can contribute to the design of novel solid-state materials made of doped Al clusters, which may ultimately be suitable for catalytic processes.

1. Introduction

There has been considerable interest in the interaction of hydrogen with light metals in order to discover inexpensive lightweight materials for hydrogen storage. For this to be successful, the interaction of hydrogen with the material must be thermodynamically and kinetically favorable.[1] This means that the barrier for dissociative adsorption of H_2 onto the materials should be relatively low, and the binding of hydrogen to the material should be only slightly exothermic. Recently, Pozzo et al.[2] found that when Ni/Ti are added as dopants on an Mg(0001) surface, the barrier for hydrogen dissociation is negligible. However, the binding energy of two hydrogen atoms on the Ti-doped surface is high, impeding diffusion away from the Ti site, whereas on the Ni-doped surface the energy barrier for diffusion is significantly reduced. This suggests that Ni is a better catalyst for Mg hydrogenation since it allows for diffusion away from the catalytic sites. Similarly, Bogdanovic and Schwickardi[3] demonstrated that doping alkali metal hydrides with a few mol% of Ti can lead to reversible decomposition at reasonable temperatures and pressures. Theoretical studies[4,5] of Ti-doped $NaAlH_4$ indicate that the Ti dopant is responsible for catalyzing H_2 chemisorption by altering the electrostatic field at the defect site when the Ti atoms are in specific local arrangements. However, the cyclable hydrogen content of these materials is low (~4%). The challenge, therefore, remains to combine high hydrogen content with favorable kinetics for adsorption and desorption of H_2. One possible alternative to these bulk materials is cluster-based materials.

The properties of metal clusters can differ significantly from those of bulk materials and are often dependent on not only the composition but also the size of the cluster. As a result, cluster-based materials are increasingly being investigated for their reactivity and catalytic activity. Experimental and theoretical studies have shown that among the small aluminum clusters, Al_7 and Al_{13} are particularly stable[6−9] because their valence electronic configurations approach closed shell "magic" configurations, as characterized by the jellium model.[10,11] It has also been proposed that adsorption of hydrogen on Al_{13} can provide the necessary electron to complete its electronic configuration and, therefore, $Al_{13}H$ may be suitable for the preparation of new cluster-assembled materials.[12−16] Among the doped aluminum clusters, the silicon-centered $Al_{12}Si$ cluster has been widely investigated;[17] however, the magnesium-centered $Al_{12}Mg$ has been less studied.[18,19] Lu et al.[19] recently reported that $Al_{12}Mg$ has icosahedral symmetry. However, our theoretical calculations[20] indicate that the $Al_{12}Mg$ cluster is a stable structure with D_{5d} symmetry due to a Jahn−Teller distortion and has a binding energy of 29.62 eV, which exists in the $^3A_{1g}$ triplet electronic state. $Al_{12}Mg$ has 38 valence electrons and, therefore, within the Jellium model might be expected to have a favorable interaction with H_2 to achieve a 40 electron closed shell configuration.

We found[20] that the binding energy of a H atom to $Al_{12}Mg$ is 2.36 eV, and the reaction (eq 1) proceeds without a barrier, in agreement with Lu et al.[19] Similarly, our previous study[21] found that addition of a H atom to the $Al_{12}X$ clusters (X = Al and Si) also proceeds without a barrier (eqs 2 and 3) and that these are exothermic reactions.

$$Al_{12}Mg + H \rightarrow Al_{12}MgH \qquad \Delta H = -2.36 \text{ eV} \qquad (1)$$

$$Al_{13} + H \rightarrow Al_{13}H \qquad \Delta H = -2.21 \text{ eV} \qquad (2)$$

$$Al_{12}Si + H \rightarrow Al_{12}SiH \qquad \Delta H = -1.77 \text{ eV} \qquad (3)$$

Moreover, Al_{13} and derivatives have been theoretically demonstrated to strongly bond significant numbers of H atoms ($Al_{12}H_{20}$ and $Al_{13}H_{13}$)[22,23] and can be useful in H storage applications. However, the interaction of hydrogen with light-metal clusters is generally characterized by high binding energies and slow kinetics that may be advantageous in the formation of stable assemblies but is less appropriate for catalytic applications and the use of clusters as a direct hydrogen storage medium. It is, therefore, of interest to investigate how doping of these clusters alters their stability and reactivity with H. We have recently[20] been investigating theoretically the reactivity of H_2 with neutral and charged X-centered aluminum clusters ($Al_{12}X$, X = Mg, Al, and Si) (eqs 4−6) and found that the lowest

---

* Corresponding author. E-mail: irene.yarovsky@rmit.edu.au.

10.1021/jp810688f CCC: $40.75

barrier for dissociative adsorption of H_2 on a neutral cluster occurs for the $Al_{12}Mg$ cluster, while the highest barrier was found to be on the closed shell $Al_{12}Si$.

$$Al_{12}Mg + H_2 \rightarrow Al_{12}MgH_2 \quad \Delta H^{\ddagger} = 0.52\ \text{eV}, \quad \Delta H = -0.41\ \text{eV} \qquad (4)$$

$$Al_{13} + H_2 \rightarrow Al_{13}H_2 \quad \Delta H^{\ddagger} = 0.80\ \text{eV}, \quad \Delta H = -0.40\ \text{eV} \qquad (5)$$

$$Al_{12}Si + H_2 \rightarrow Al_{12}SiH_2 \quad \Delta H^{\ddagger} = 1.37\ \text{eV}, \quad \Delta H = +0.24\ \text{eV} \qquad (6)$$

The barriers for H_2 desorption from the dihydrogenated clusters are generally quite substantial. Our study also found that there was a strong linear correlation between barrier heights ($\Delta H^{\ddagger}$) and reaction enthalpy, indicating that these reactions are strongly thermodynamically driven. Further to this, we found that while there was very little correlation between frontier orbital energies and $\Delta H^{\ddagger}$, there were much closer relationships between cluster distortion energies and $\Delta H^{\ddagger}$.

In this work we extend our investigation of H_2 interactions with $Al_{12}X$ clusters to include reaction profiles for H−H bond homolysis by one and two clusters.

2. Computational Procedures

Spin-polarized calculations were performed at the Perdew−Burke−Ernzerhof/double numerical polarized (PBE/DNP) level with the DMol^3 program,[24,25] which we have tested thoroughly for this application against benchmark levels of theory.[21] All geometries were calculated with the PBE functional[26] using the DNP basis set that includes a *d*-type polarization function on heavy atoms and a *p*-type polarization function on hydrogen. It was previously shown that an all electron basis set with the addition of *d* functions is essential for a proper description of high-valence Al atoms.[27] The computationally economical DNP basis set is comparable in size to the Gaussian-type 6-31G(d,p) basis set and has been found to give similar performance for Al cluster geometries and binding energies.[21]

Atom-centered grids were used for the numerical integration with the "fine" option in DMol^3 that includes about 2000 grid points for each atom. Self-consistent field (SCF) convergence was set so that the rms change in the electronic density was less than 2.7×10^{-5} eV. Convergence tolerance for geometry optimization was 2.7×10^{-4} eV for energy, 0.054 eV/Å for force, and 0.005 Å for displacement. The orbital cutoff was set to 15.0 Å, and the thermal occupation was set at 0.136 eV. No symmetry constraints were applied to the systems investigated, and vibrational frequency analysis was performed to characterize all stationary points as true minima or transition structures. All energies determined in the present study have been corrected for zero-point vibrational energy.

3. Results and Discussion

The first group of reactions we consider in this work involve homolytic H_2 bond cleavage leading to the formation of $Al_{12}XH$ and H atom (eqs 7−9).

$$Al_{12}Mg + H_2 \rightarrow Al_{12}MgH + H \qquad \Delta H = +1.91\ \text{eV} \qquad (7)$$

$$Al_{13} + H_2 \rightarrow Al_{13}H + H \qquad \Delta H = +2.06\ \text{eV} \qquad (8)$$

$$Al_{12}Si + H_2 \rightarrow Al_{12}SiH + H \qquad \Delta H = +2.50\ \text{eV} \qquad (9)$$

Reactions 7−9 are strongly endothermic. Homolytic bond cleavage of H_2 requires 4.27 eV, but formation of $Al_{12}XH$ returns only −1.77 to −2.36 eV (eqs 1−3) leading to the large endothermicities for these reactions. We have carried out an extensive search of the potential energy surface along the reaction coordinate and have not been able to locate a transition state for these reactions.

The bond homolysis processes (eqs 7−9) involve the same set of reactants as the dissociative adsorption processes (eqs 4−6), respectively. All of these reactions begin with the same set of $Al_{12}X$ and H_2 orbitals and differ only in the orientation of the molecules and, therefore, the orbitals with respect to one another. Previously, we noted for the adsorption reactions (eqs 4−6) that while overlap of the highest occupied molecular orbital (HOMO) of the cluster with the lowest unoccupied molecular orbital (LUMO) of H_2 should lead to the weakening of the H−H bond during the process, there was no clear correlation between the ($Al_{12}X^{HOMO}-H_2^{LUMO}$) difference and the barriers. This is in agreement with the earlier work of Upton and co-workers[28,29] for the Al_6/H_2 system. The absence of barriers for reactions 7−9 also demonstrates the relative unimportance of the $Al_{12}X^{HOMO}-H_2^{LUMO}$ gap for these interactions. However, both our previous study and that of Upton identified a more important contribution arising from the significant changes in the cluster populations necessary to initially minimize repulsive interactions between the cluster and H_2 and then subsequently to enable formation of the new Al−H bonds. This reorganization of the electronic populations can be linked to the distortion energy of the clusters for the $Al_{12}X/H_2$ systems. We note here that the HOMO of the $Al_{12}Mg$ cluster (Figure 1a) has axial symmetry[30] and is, therefore, better suited to an axial σ-type interaction rather than the pseudo-π-type interaction required for reaction 4. Consequently, a σ-type interaction along the axis of the cluster, as in reaction 7, results in little distortion of the cluster orbitals and, therefore, eliminates this contribution to the interaction. In comparison, while the HOMO of Al_{13} has some axial character, it is more delocalized than observed for the $Al_{12}Mg$ cluster. The HOMO of $Al_{12}Si$ has essentially no axial character and is largely delocalized among the Al cage atoms, and we might, therefore, expect barriers for these reactions. However, for both Al_{13} and $Al_{12}Si$ there are axial orbitals (162 and 157, respectively) close in energy to the HOMO of these clusters that can efficiently overlap with LUMO of H_2 and, therefore, minimize repulsive interactions

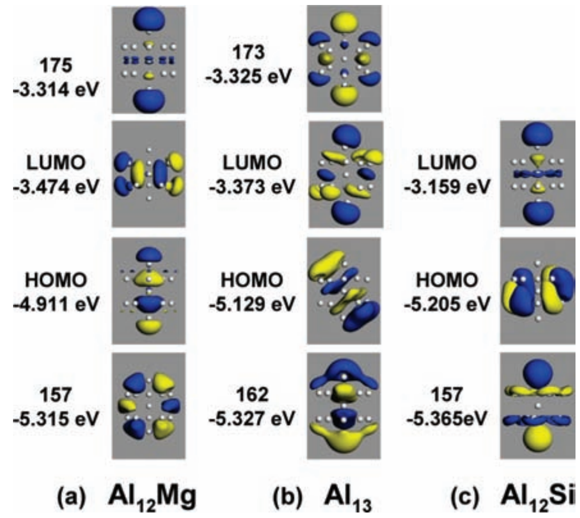

Figure 1. Frontier and key orbitals of (a) $Al_{12}Mg$, (b) Al_{13}, and (c) $Al_{12}Si$.

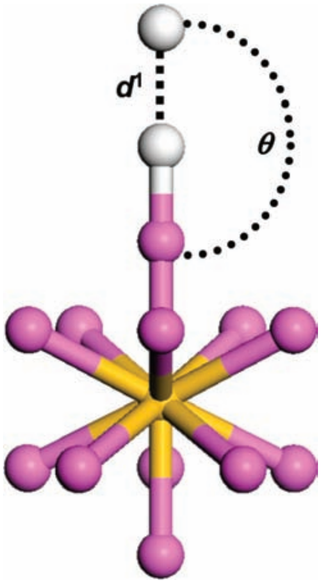

Figure 2. Definitions of key calculated distance and angle for reactions 7–9.

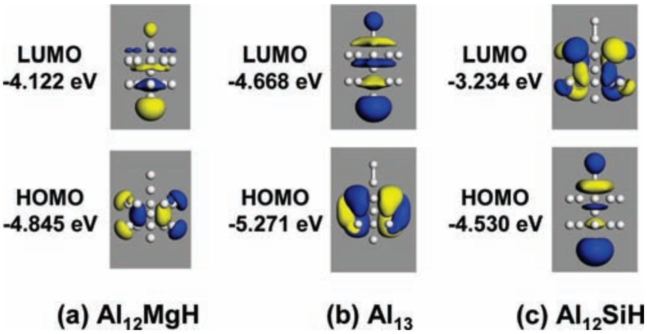

Figure 3. Frontier orbitals of $Al_{12}XH$ (X = Mg, Al, and Si) clusters.

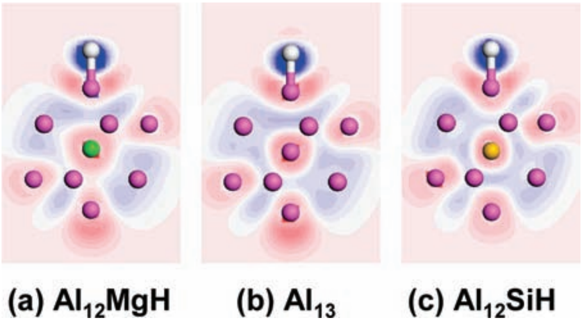

Figure 4. Electron deformation densities for the $Al_{12}XH$ species.

between the clusters and H_2, thus, explaining the absence of barriers for H adsorption in these systems.

Clearly reactions 7−9 are energetically unfavorable and will only occur at high temperatures, making them of limited practical application. However, the reverse reactions in which H atom abstracts hydrogen from $Al_{12}XH$ also proceed without barriers and are highly exothermic. We find that for distances (d^1) of <2.45 Å (Figure 2), the interaction between H atom and the $Al_{12}XH$ clusters is sufficiently strong that geometry optimization leads to the formation of H_2 and $Al_{12}X$. To further explore this process we have investigated the angular dependence for the approach of a hydrogen atom to the $Al_{12}XH$ clusters (Figure 2). We find that the hydrogen atom also abstracts hydrogen from $Al_{12}XH$ for approach angles (θ) of 150, 135, and 120° ($d^1 = 2.0$ Å). However, with an approach angle of 90°, the interaction between the cluster and the "abstracting" hydrogen is greater than that between the two hydrogen atoms, and the reactions lead to the formation of $Al_{12}XH_2$. These results have significant implications for hydrogen storage applications. In particular, while our earlier study[22] of A_{12} and Al_{13} revealed that these clusters can strongly bind 20 and 12 hydrogen atoms, respectively, experimental studies[8,12] of H atom reactions with Al_{13} have so far only revealed the formation of $Al_{13}H_n$ with $n = 1-3$. We can see that both the H addition and H abstraction (reverse of eq 8) are barrierless exothermic processes and, therefore, will generally be competing reactions under experimental conditions. The observation of only $Al_{13}H_n$ ($n = 1-3$) most likely represents a "steady state" for the competing reactions under the specific experimental conditions. A similar situation should occur for the $Al_{12}Mg$/H and $Al_{12}Si$/H systems. However, for the magnesium-doped system, the enthalpy for H atom addition is greater (0.45 eV) than the enthalpy for H atom abstraction, which should favor the formation of $Al_{12}MgH_n$ over H abstraction. The reverse is true for the silicon-doped system, where ΔH for abstraction is greater (0.73 eV) than H atom addition, and so abstraction should be favored. This indicates that any $Al_{12}X$-based hydrogen storage technology that involves predissociation of H_2 will be limited by the competing addition and abstraction reactions. However, the H abstraction reactions may provide the basis for a thermodynamically favorable H_2 release mechanism from H-loaded $Al_{12}X$ clusters.

Figure 3 displays the frontier orbitals for the $Al_{12}XH$ monohydrides. In the case of $Al_{12}Mg$ and Al_{13}, the HOMOs are delocalized around the cluster metal atoms and do not include the H atom. However, the LUMOs of these species are delocalized along the principal axis, which includes the H atom. The reverse is true for $Al_{12}SiH$, where the LUMO is delocalized around the cluster Al atoms, but the HOMO has axial symmetry. However, in all three cases the axial frontier orbitals are suitable for overlap with the singly occupied 1s orbital of H atom. Figure 4 displays the slice of the electron deformation densities for the $Al_{12}XH$ species. Clearly shown for all three species is the high concentration of charge density around the H atoms in agreement with earlier studies. The large concentration and extent of density around the H atom, compared with that of the cluster cage atoms, also accounts for the small angular dependence for the abstraction process compared with addition of a second hydrogen atom to the cluster.

Having established that homolytic bond cleavage reactions 7−9 are highly endothermic, the next stage of the study was to investigate the axial interaction of two $Al_{12}X$ clusters with a H_2 molecule positioned between them (10−12) as shown in Figure 5a.

$$2Al_{12}Mg + H_2 \rightarrow 2Al_{12}MgH \qquad \Delta H = -0.58\ \text{eV} \qquad (10)$$

$$2Al_{13} + H_2 \rightarrow 2Al_{13}H \qquad \Delta H = -0.15\ \text{eV} \qquad (11)$$

$$2Al_{12}Si + H_2 \rightarrow 2Al_{12}SiH \qquad \Delta H = +0.73\ \text{eV} \qquad (12)$$

For values of $d^1 \geq 3.0$ Å there is essentially no interaction between the clusters and the H_2 molecule, as demonstrated by the negligible energy difference (<0.02 eV) between the aggregate and the sum of the energies of the individual species. However, for $Al_{12}Mg$ with $d^1 < 3.0$ Å the interaction is sufficiently strong[31] that geometry optimization leads to each cluster being initially drawn toward the nearest respective H atom, followed by spontaneous dissociation of the H_2 and formation of two separate $Al_{12}MgH$ species. The H^1-H^2 distance (d^2) of H_2 and the Al−Mg distance for each of the $Al_{12}Mg$ clusters in the initial configuration are equal to those observed for the isolated species, and the separation between the clusters (d^3) is 5.751 Å (Figure 6). As the process continues, the distances between the cluster atoms and the hydrogen atoms (d^1) shorten, and as a consequence the distance between the clusters (d^3) also shortens and reaches a minimum value of ~4.583 Å before increasing again to a value of ~5.75 Å after the dissociation has occurred. The final values of d^1 (1.597 Å) and Al−Mg (2.573 Å) are those of isolated atop isomers of $Al_{12}MgH$. A similar process is observed for the interaction of H_2 with two Al_{13} clusters; however, while the final arrangement resembles structurally that of two $Al_{13}H$ species, this stationary point does not represent a minimum on the potential energy surface. For the $Al_{12}Si$ system, the interaction is repulsive, and the energy minimization process leads to the isolated reactants.

As we noted earlier, dissociation of the H_2 molecule is a highly endothermic process $\Delta H = +4.27$ eV; however, the enthalpy of the spontaneous dissociation (eq 10) is $\Delta H = -0.58$ eV. The energy balance is achieved by the fact that the reaction of H atom with $Al_{12}Mg$ (eq 1), to give an atop isomer of $Al_{12}MgH$, is an exothermic reaction ($\Delta H = -2.36$ eV) that also proceeds without a barrier, and we receive two molecules of $Al_{12}MgH$ for each H_2 molecule dissociated (eq 10). In comparison, the reaction of H_2 with a single $Al_{12}Mg$ cluster (eq 4) is also an exothermic process ($\Delta H = -0.41$ eV); however, this reaction proceeds via a barrier ($\Delta H^{\ddagger} = +0.52$ eV). For the $2Al_{13}/H_2$ system the reaction is calculated to be only slightly exothermic, while for the $2Al_{12}Si/H_2$ system the reaction is strongly endothermic.

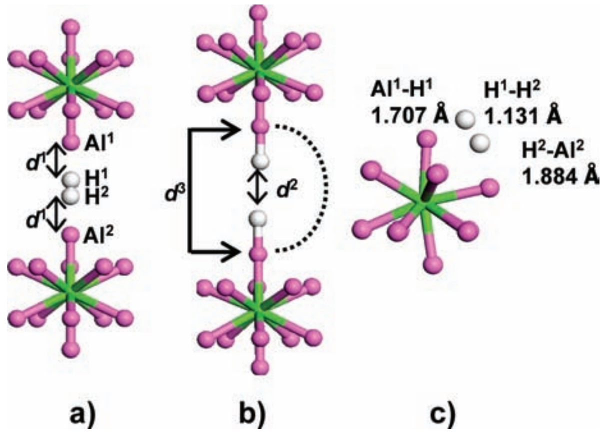

Figure 5. (a,b) Initial and final structures for reaction 10 with definitions of key calculated distances and angle. (c) Transition structure for reaction 4.

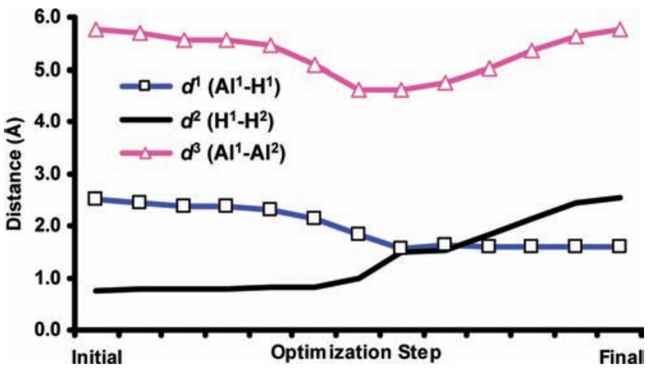

Figure 6. Evolution of key distances during the course of the reaction 10.

To better understand the spontaneity of the $2Al_{12}Mg/H_2$ reaction, we have analyzed reactions 4 and 10 in terms of the orbital interactions and the electron deformation densities. As shown above, the interaction of a single cluster in the axial arrangement is too weak to lead to dissociation of H_2; however, when there is a concerted interaction between the HOMO orbitals of two $Al_{12}Mg$ clusters with the LUMO of H_2, this initiates the dissociation process. Smaller contributions to the energy lowering are also achieved by the overlap of other occupied axial orbitals of $Al_{12}Mg$ with the unoccupied orbitals of H_2. We also note that while the symmetry of the LUMO of $Al_{12}Mg$ is not suited to overlap with the HOMO of H_2, orbital 175, which is only slightly higher in energy, provides the necessary symmetry (Figure 1a). As noted earlier, we observe significant reorganization of cluster orbitals for H_2 dissociation on a single $Al_{12}Mg$, which is also evident from the significant distortion of the cluster geometry in the transition structure (Figure 5c). However, for the spontaneous dissociation between two $Al_{12}Mg$ clusters we observe that, as the reaction proceeds, the “axial” orbitals generally lower in energy as the H−H bond is broken and the new Al−H bonds are formed. The concerted lowering in energy of these orbitals drives the reaction toward the product configuration. Additionally, orbitals not possessing axial symmetry remain relatively undisturbed throughout the course of the reaction and, therefore, do not make a “repulsive” contribution to energy change.

The spontaneous dissociation of reaction 10 involves σ-type overlap between the orbitals of the $Al_{12}X$ clusters and H_2. In comparison, the dissociative adsorption of H_2 onto a single cluster (eq 4) necessitates a sideways approach and, therefore, a π-type interaction. The HOMO orbital of $Al_{12}Mg$ does not possess the required symmetry to facilitate this process. Orbital 157 at −5.315 eV is the highest of the $Al_{12}Mg$ occupied orbitals involved in this process. Clearly there is a larger energy separation between key orbitals for reaction 4 than observed for reaction 2, and this contributes to the observed reaction barrier. We also note that contributions are also observed from lower energy $Al_{12}Mg$ occupied orbitals. However, the high degree of delocalization and larger energy separation from the unoccupied H_2 orbitals make these interactions relatively weak.

The interaction of a single H atom with an $Al_{12}X$ cluster is characterized by a significant transfer of electron density from the cluster to the H atom, similar to Al_{13}/Al_{12}.[14] Likewise, in the reaction of H_2 with two $Al_{12}Mg$ clusters, we observe significant transfer of electron density from each cluster to the nearest respective H atom, as indicated by plots of the electron deformation density (Figure 7a). We can see for reaction 10 that initially there is strong localization of charge around the H atoms corresponding to the H−H bond and symmetrical distribution of density delocalized across the framework formed by the metal atoms of each cluster. As the reaction proceeds, there is a transfer of electron density from the H−H bonding region to the zones between the H atoms and the clusters. In the final arrangement, significant density is localized between the H atoms and the atop Al atoms of the respective clusters. As a consequence, there are further decreases in density around the axial atoms of the

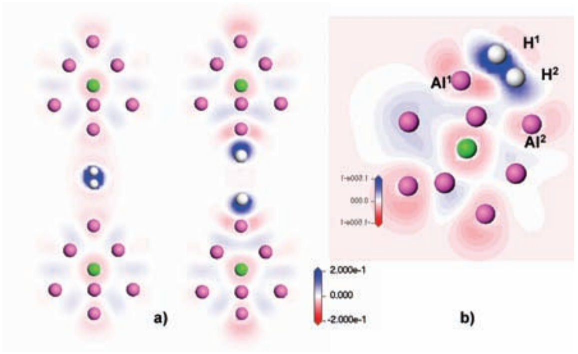

Figure 7. Electron deformation density for (a) the initial and final structures of reaction 2 and (b) the transition structure of reaction 4.

clusters, indicating that these atoms make significant contributions to the Al−H bond. Our studies indicate that doping of the cluster with an electropositive atom (Mg) enables transfer of electron density to the Al cage, which enhances H_2 dissociation.

In the spontaneous process (reaction 10) each cluster donates an equivalent amount of electron density to its respective H atom. However, for reaction 4 involving a single $Al_{12}Mg$, all of the electron density must be contributed from just one cluster. Figure 7b displays the electron deformation density for the $Al_{12}Mg/H_2$ transition state. Clearly identified are both the significant electron density remaining between the hydrogen atoms and the initial stages of the transfer of density from the cluster to the H atoms, as demonstrated by the decreased electron density around the neighboring Al atoms. Particularly evident is the significant decrease in density around the Al^1 aluminum (Figure 7b). The electron deformation densities also clearly illustrate that one of the major differences between the spontaneous process (eq 10) and the barrier process (eq 4) is the different requirements for electron transfer from the clusters to the H atoms. In particular, the transfer of density in reaction 4 is less uniform with Al^1 required to transfer density to both the atop hydrogen (H^1) and the bridge hydrogen (H^2), while Al^2 provides density solely to H^2. The transfer of electrons to the H atoms significantly disrupts the Al cage density and contributes to the activation energy of reaction 10.

We have also investigated the angular dependence of the reaction and found that for angles of up to 150° between the clusters, along the principal axis (Figure 5), there is still spontaneous dissociation of H_2 to give two $Al_{12}MgH$ species. This is possible because sufficient overlap of the cluster "axial" orbitals with the H_2 orbitals can still be achieved to initiate the dissociation. However, for angles of 120° and 90° between the clusters, interaction between the orbitals of the clusters dominates, which results in merging of the clusters, with the hydrogen atoms adsorbed on the surface of the aggregate.

Clearly in the gas phase, the probability of occurrence of our trimolecular spontaneous process (eq 10) is quite low. However, the aim of this work is to demonstrate that for specific arrangements of clusters, it is possible to achieve spontaneous dissociation of H_2. Our ongoing research will investigate the embedding/deposition of $Al_{12}X$ clusters in an "inert" material, such as a carbon framework. This will also prevent possible coalescence of the metal clusters in a condensed phase.

4. Conclusions

We have investigated axial interactions of H_2 with $Al_{12}X$ (X = Mg, Al, and Si) clusters and found that homolytic dissociation, leading to the $Al_{12}XH$ and H atom, proceeds without a barrier but is an extremely endothermic process. However, dissociation of a H_2 molecule between closely spaced $Al_{12}Mg$ clusters proceeds spontaneously. The linear arrangement of $Al_{12}Mg$ clusters and H_2 allows optimal overlap of the "axial" orbitals of the clusters and H_2, enhancing transfer of electron density to the H atoms. Doping of the cluster with an electropositive atom (Mg) enables transfer of electron density to the Al cage, which enhances H_2 dissociation. Further to this, spreading the electron density demand of the H atoms over two clusters rather than one, enables the process to proceed without an energy barrier. While the binding of hydrogen to these clusters is too strong to be of direct application in catalysis, the information gained can contribute to the design of novel solid-state materials made of Al-doped clusters, which may ultimately be suitable for catalytic processes.

Acknowledgment. We gratefully acknowledge the award of an Australian Research Council Discovery Grant to carry out this work. We also gratefully acknowledge allocation of computing time from the National Facility of the Australian Partnership for Advanced Computing (APAC). We would also like to thank Dr. Bernard Delley and Dr. Alexander Goldberg for helpful discussions.

References and Notes

(1) Bhatia, S. K.; Myers, A. L. *Langmuir* **2006**, *22*, 1688–1700.
(2) Pozzo, M.; Alfè, D.; Amieiro, A.; French, S.; Pratt, A. *J. Chem. Phys.* **2008**, *128*, 094703.
(3) Bogdanovic, B.; Schwickardi, M. *J. Alloys Compd.* **1997**, *253−4*, 1–9.
(4) Chaudhuri, S.; Muckerman, J. T. *J. Phys. Chem. B* **2005**, *109*, 6952–6957.
(5) Chaudhuri, S.; Graetz, J.; Ignatov, A.; Reilly, J. J.; Muckerman, J. T. *J. Am. Chem. Soc.* **2006**, *128*, 11404–11415.
(6) Rao, B. K.; Jena, P. *J. Chem. Phys.* **1999**, *111*, 1890–1904.
(7) Ahlrichs, R.; Elliott, S. D. *Phys. Chem. Chem. Phys.* **1998**, *1*, 13–21.
(8) Cox, D. M.; Trevor, D. J.; Whetten, R. L.; Kaldor, A. *J. Phys. Chem.* **1988**, *92*, 421–429.
(9) Taylor, K. J.; Pettiette, C. L.; Craycraft, M. J.; Chesnovsky, O.; Smalley, R. E. *Chem. Phys. Lett.* **1988**, *152*, 347–352.
(10) Knight, W. D.; Clemenger, K.; de Heer, W. A.; Saunders, W. A.; Chou, M. Y.; Cohen, M. L. *Phys. Rev. Lett.* **1984**, *52*, 2141–2143.
(11) Chou, M. Y.; Cohen, M. L. *Phys. Lett.* **1986**, *113A*, 420–424.
(12) Burkart, S.; Blessing, N.; Klipp, B.; Müller, J.; Ganteför, G.; Seifert, G. *Chem. Phys. Lett.* **1999**, *301*, 546–550.
(13) Kawamura, H.; Kumar, V.; Sun, Q.; Kawazoe, Y. *Phys. Rev. B* **2001**, *65*, 045406.
(14) Mañanes, A.; Duque, F.; Méndez, F.; López, M. J.; Alonso, J. A. *J. Chem. Phys.* **2003**, *119*, 5128–5141.
(15) Yarovsky, I.; Goldberg, A. *Mol. Simul* **2005**, *31*, 475–481.
(16) Han, Y.-K.; Jung, J.; Kim, K. H. *J. Chem. Phys.* **2005**, *122*, 124319.
(17) Kumar, V.; Bhattacharjee, S.; Kawazoe, Y. *Phys. Rev. B: Condens. Matter Mater. Phys.* **2000**, *61*, 8541–8547.
(18) Charkin, O. P.; Charkin, D. O.; Klimenko, N. M.; Mebel, A. M. *Faraday Discuss.* **2003**, *124*, 215.
(19) Lu, Q. L.; Jalbout, A. F.; Luo, Q. Q.; Wan, J. G.; Wang, G. H. *J. Chem. Phys.* **2008**, *128*, 224707.
(20) Henry, D. J.; Yarovsky, I. *J. Phys. Chem. A* **2009**, *113*, 2565−2571.
(21) Henry, D. J.; Varano, A.; Yarovsky, I. *J. Phys. Chem. A* **2008**, *112*, 9835–9844.
(22) Goldberg, A.; Yarovsky, I. *Phys. Rev. B: Condens. Matter Mater. Phys.* **2007**, *75*, 195403.
(23) Jung, J.; Han, Y.-K. *J. Chem. Phys.* **2006**, *125*, 064306.
(24) Delley, B. *J. Chem. Phys.* **1990**, *92*, 508–517.

(25) Delley, B. *J. Chem. Phys.* **2000**, *113*, 7756.

(26) Perdew, J. P.; Burke, K.; Ernzerhof, M. *Phys. Rev. Lett.* **1996**, *77*, 3865–3868.

(27) Fowler, J. E.; Ugalde, J. M. *Phys. Rev. A: At., Mol., Opt. Phys.* **1998**, *58*, 383–388.

(28) Upton, T. H. *Phys. Rev. Lett.* **1986**, *56*, 2168–2171.

(29) Upton, T. H.; Cox, D. M.; Kaldor, A. In *The Physics and Chemistry of Small Clusters*; Jena, P., Ed.; Plenum: New York, 1987.

(30) The singly occupied orbitals of $Al_{12}Mg$ are marginally lower in energy ($E = -4.941$ eV) and more delocalized than the HOMO.

(31) At $d = 2.5$ Å, the total energy of the aggregate is 0.05 eV less than the sum of the energies of the individual species.

JP810688F